Supporting Information for:

# Direct Ladderization of Cyclooctatetraene-containing, Processable Conjugated Ladder Polymers from Annulated bis-Zirconacyclopentadienes

August J. Rothenberger,[1] Harrison M. Bergman,[1] He Li,[2,3] Miao Qi,[2] Yunfei Wang,[2] Yi Liu,*[2,3] and T. Don Tilley*[1,4]

[1]Department of Chemistry, University of California, Berkeley, Berkeley, California, 94720, United States
[2]Molecular Foundry, Lawrence Berkeley National Laboratory, Berkeley, California, 94720, United States
[3]Materials Sciences Division, Lawrence Berkeley National Laboratory, Berkeley, California, 94720, United States
[4]Chemical Sciences Division, Lawrence Berkeley National Laboratory, Berkeley, California, 94720, United States

## General Details

Unless otherwise specified, all manipulations were carried out under a nitrogen atmosphere using standard Schlenk techniques or in inert atmosphere gloveboxes filled with nitrogen. Toluene was dried using a JC Meyers Phoenix SDS solvent purification system and stored over 3Å molecular sieves. Benzene-*d*6 was degassed with three freeze-pump-thaw cycles then was stored over 3Å molecular sieves. Zirconacyclopentadiene (zirconacycle) precursors **1**, **3**, and **4** were prepared as previously described in literature.[1] All other reagents were purchased from commercial suppliers and used without further purification. All column chromatography was carried out using Fisher Chemical 40–63μm, 230–400 mesh silica gel. NMR spectra for all compounds were recorded at 25 °C using Bruker Avance 500 MHz spectrometers as well as a JEOL ECZL400S 400 MHz spectrometer. Chemical shifts (δ) are recorded in ppm using solvent residual signals as references for $^{1}$H NMR (5.32 ppm for dichloromethan-*d2*) and $^{13}$C (53.84 ppm for dichloromethane-*d2*). $^{19}$F NMR spectra were referenced against hexaflurobenzene (-164.9 ppm in benzene-*d6*).

Size exclusion chromatography (SEC) was performed using a Malvern Panalytical OMNISEC instrument with THF as eluent and dual right-angle and low-angle light scattering detectors to determine dn/dc. Samples were dissolved in THF at a concentration of 2 mg/mL and eluted through the instrument at a flow rate of 1 mL/min. Differential Scanning Calorimetry (DSC) was performed using a TA Instruments Q200/RCS90. Thermogravimetric analysis (TGA) was performed using a TA Instruments Q5500 TGA-MS. Porosimetry was performed using a Micromeretics Tristar II 3020. Samples were activated at 120 °C and 150 mtorr for 24 h before porosimetry analysis. Pore size distributions were determined by NLDFT using a carbon slit model. Mass spectra were acquired on a Bruker RapifleX MALDI-TOF/TOF spectrometer using a dithranol matrix. Thin-film casting and characterization is described in further detail on page 18. Photophysical spectra was acquired using a Shimadzu UV-2600 i UV-Vis spectrophotometer, a Cary Eclipse Fluorescence spectrophotometer, and a Bruker Vertex 80 FTIR Spectrometer with a Platinum ATR. UV-Vis spectra and fluorescence spectra were collected in $CH_2Cl_2$ at a concentration of 25-50 μg/mL. Cyclic voltammetry was acquired using an BASi EC Epsilon potentiostat. Polymer characterization data was acquired from samples reacted for 2 hours, unless otherwise noted.

**Synthesis of COT Polymers**

To a solution of bis-zirconacycle (**3** or **4**) and 1,4-diazabicyclo[2.2. 2]octane (10 equiv.) in toluene (5 mg/mL) was added anhydrous $CuCl_2$ (6 equiv.) and the reaction mixture was stirred vigorously for 2 h at room temperature. It was then eluted through a plug of silica with toluene and the solvent removed by rotary evaporation. The remaining precipitate was dissolved in a minimal amount of dichloromethane, which was added dropwise to methanol while stirring to suspend a pale-yellow precipitate. The precipitate was collected by centrifuging the suspension, decanting the supernatant, and drying the resulting solid on a high-vacuum line.

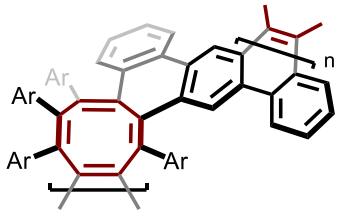


**Poly-3**. From 200 mg (0.154 mmol) of **3**. Isolated as a pale yellow powder (0.111 g, 84%). $^{1}$H NMR (dichloromethane-*d2*, 500 MHz) δ 10.56-5.54 (br, 26 H), 1.50-0.50 (br, 36 H). $^{13}$C NMR (dichloromethane-*d2*, 125 MHz) δ 150.31, 130.75, 125.24, 34.82, 31.41, 30.11. $M_{n,\ RALS/LALS}$ = 29.7 kg/mol, Đ = 1.52.

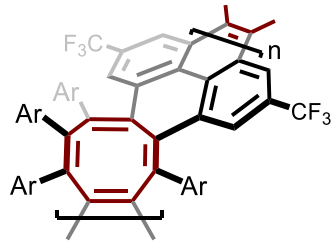


**Poly-4**. From 200 mg (0.147 mol) of **4**. Isolated as a pale yellow powder (0.109 g, 81%). $^{1}$H NMR (dichloromethane-*d2*, 500 MHz) δ 9.73-5.76 (br, 20 H), 1.60-0.38 (br, 36 H). $^{13}$C NMR (dichloromethane-*d2*, 125 MHz) δ 151.18, 131.39, 130.45, 129.38, 128.57, 125.65, 34.78, 31.31. $^{19}$F NMR (dichloromethane-*d2*, 376 MHz) δ -63.15, -68.86, -64.56, -64.71, -65.14, -65.56. $M_{n,\ RALS/LALS}$ = 26.5 kg/mol, Đ = 1.22.

**Optimization of Ligand for COT Formation**

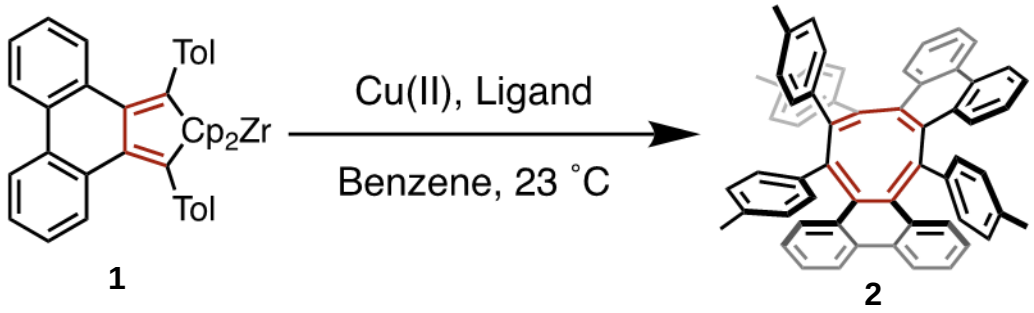


**1** **2**

Compound **1** (0.005 g, mmol) was dissolved benzene-*d6* (1 mL) and added to a vial with Cu(II) (3 equiv.), ligand (5 equiv.), and trimethoxybenzene as an internal standard. The reaction mixture was stirred for 2 hours at room temperature then filtered through celite. The reaction yield of **2** was determined by quantitative $^{1}$H NMR spectroscopy with 1,3,5-trimethoxybenzene as an internal standard. The NMR spectra for the product matched previously reported data.[1]

| **Cu(II)** | **Ligand** | **Yield** |
|---|---|---|
| $CuCl_2$ | none | 73% |
| $CuCl_2$ | pyridine | 87% |
| $CuCl_2$ | DMAP | 79% |
| $CuCl_2$ | 4-cyanopyridine | 75% |
| $CuCl_2$ | pentafluoropyridine | 24% |
| **$CuCl_2$** | **DABCO** | **93%** |
| $CuCl_2$ | $NBu_4Cl$ | 60% |
| $CuCl_2$ | 2,2'-bipy | 80% |
| $CuCl_2$ | $PPh_3$ | 79% |

**Table S1**. Optimization conditions for synthesis of **2**.

## NMR Spectra

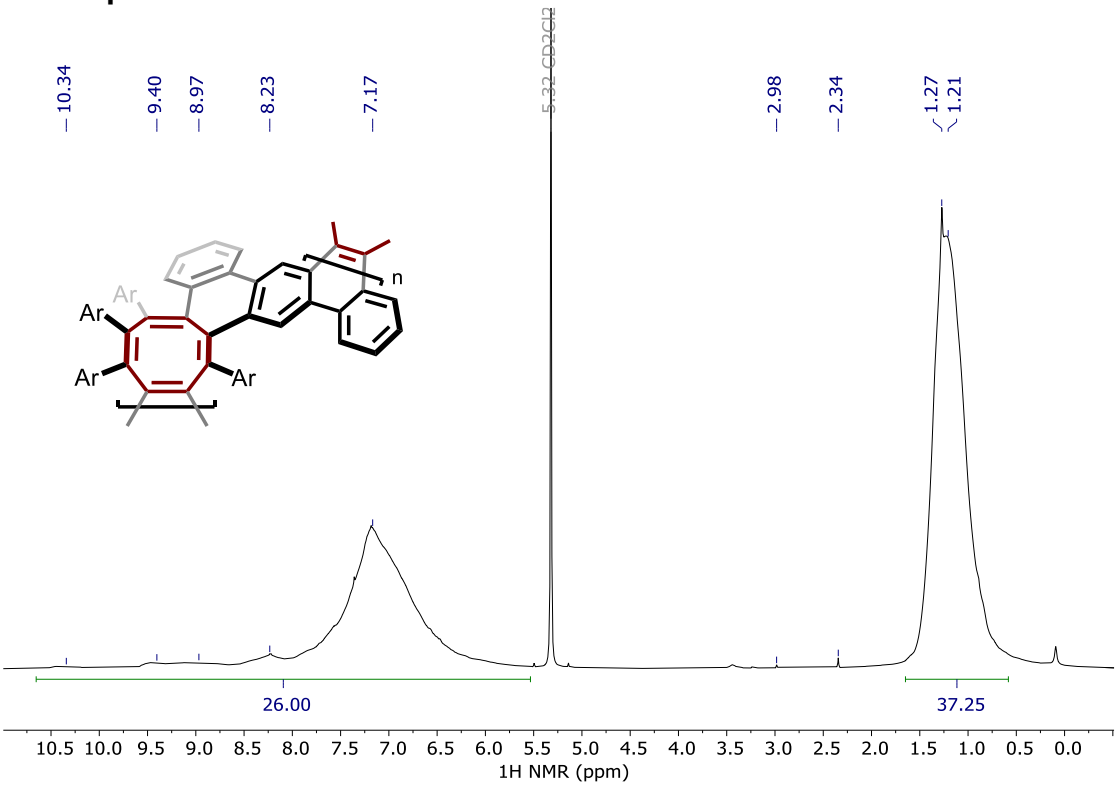


**Figure S1.** $^{1}$H NMR Spectrum (dichoromethane-*d2*, 500 MHz) of **Poly-3**

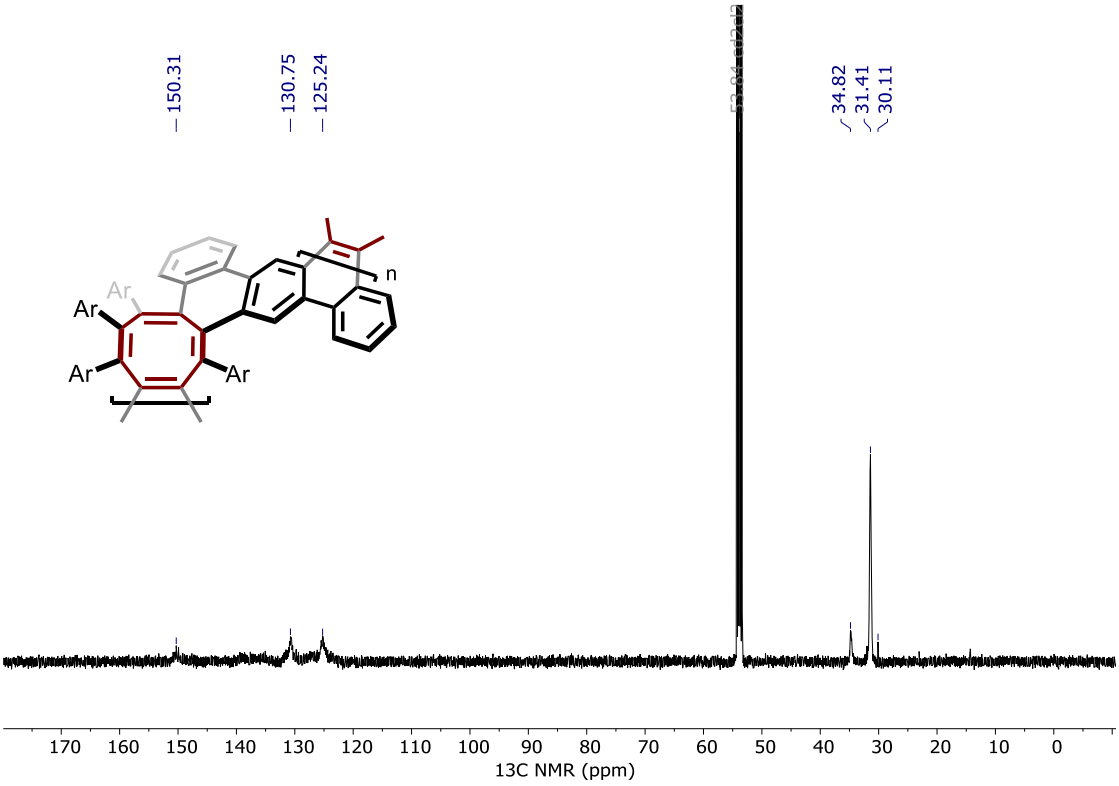


**Figure S2.** $^{13}$C NMR Spectrum (dichoromethane-*d2*, 125 MHz) of **Poly-3**

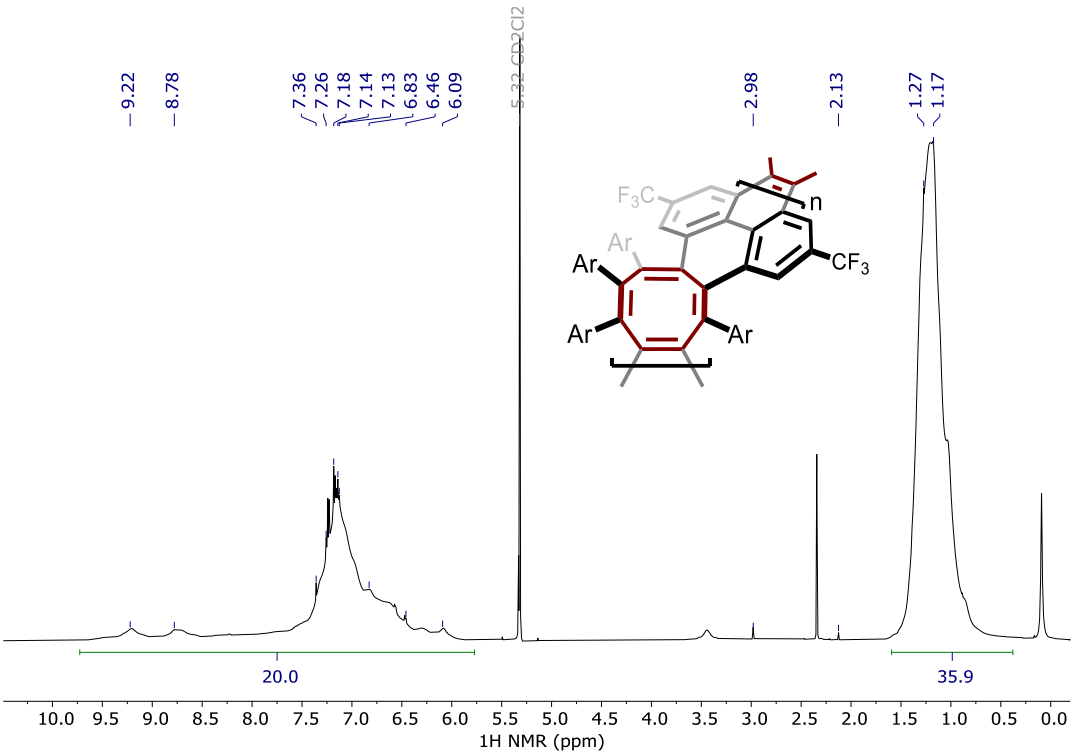


**Figure S3.** $^{1}$H NMR Spectrum (dichoromethane-*d2*, 500 MHz) of **Poly-4**

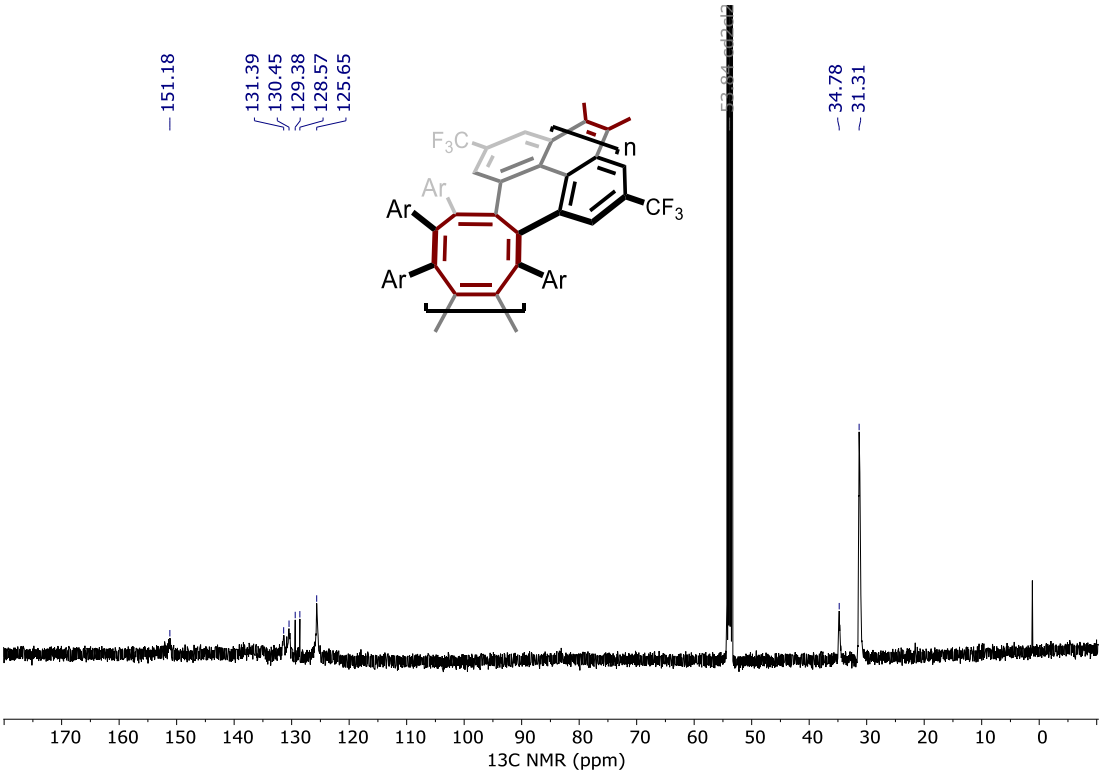


**Figure S4.** $^{13}$C NMR Spectrum (dichoromethane-*d2*, 125 MHz) of **Poly-4**

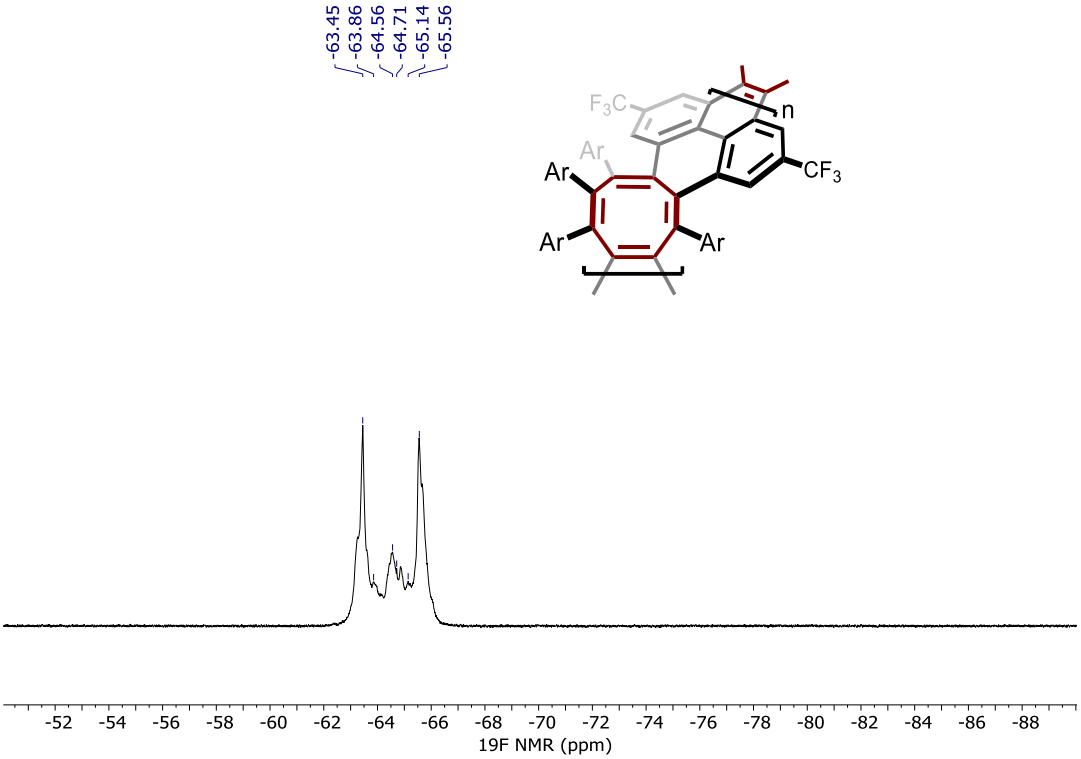


**Figure S5.** $^{19}$F NMR Spectrum (benzene-*d6*, 376 MHz) of **Poly-4**

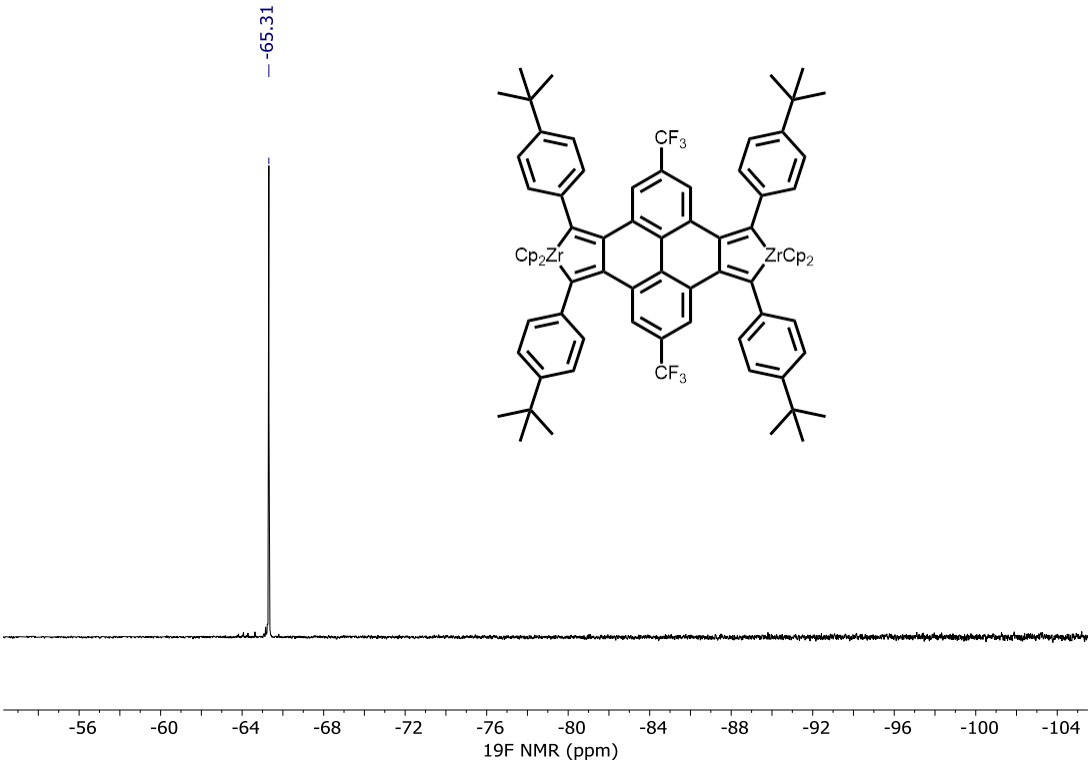


**Figure S6.** $^{19}$F NMR Spectrum (benzene-*d6*, 376 MHz) of **4**

**Mass Spectrometry**

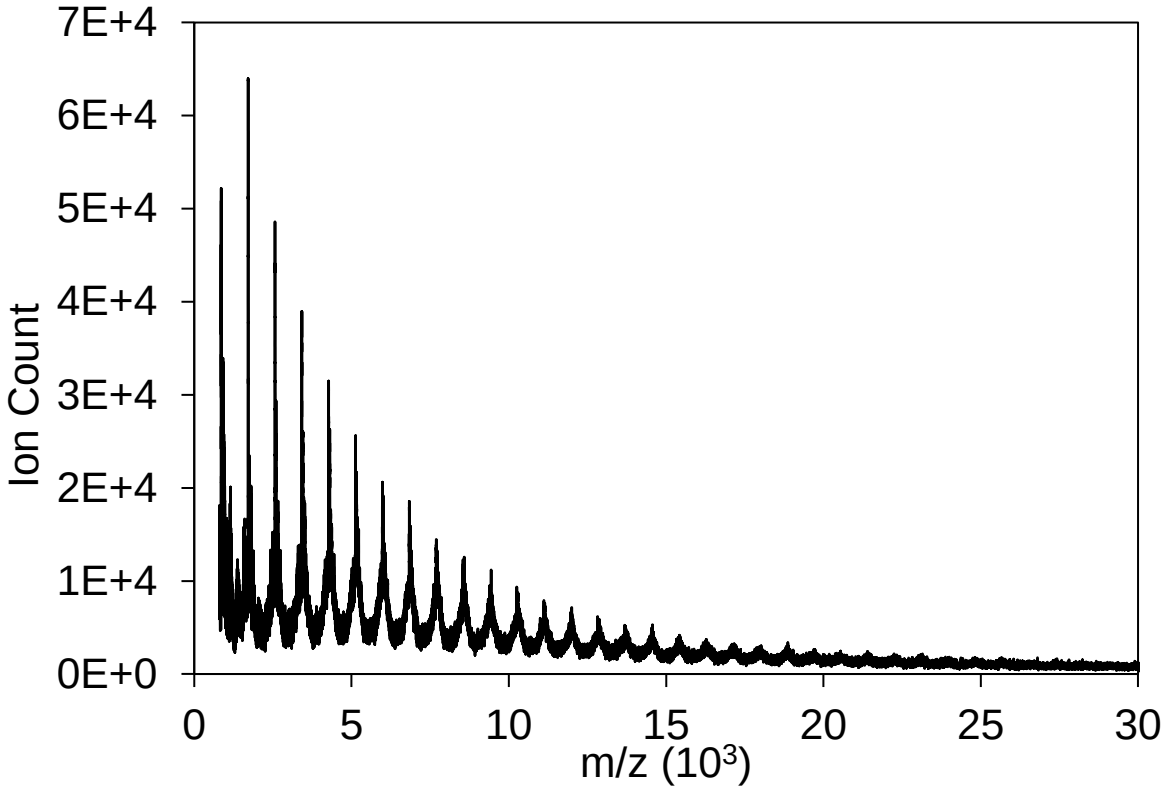


**Figure S7.** MALDI-TOF spectrum of **Poly-3**

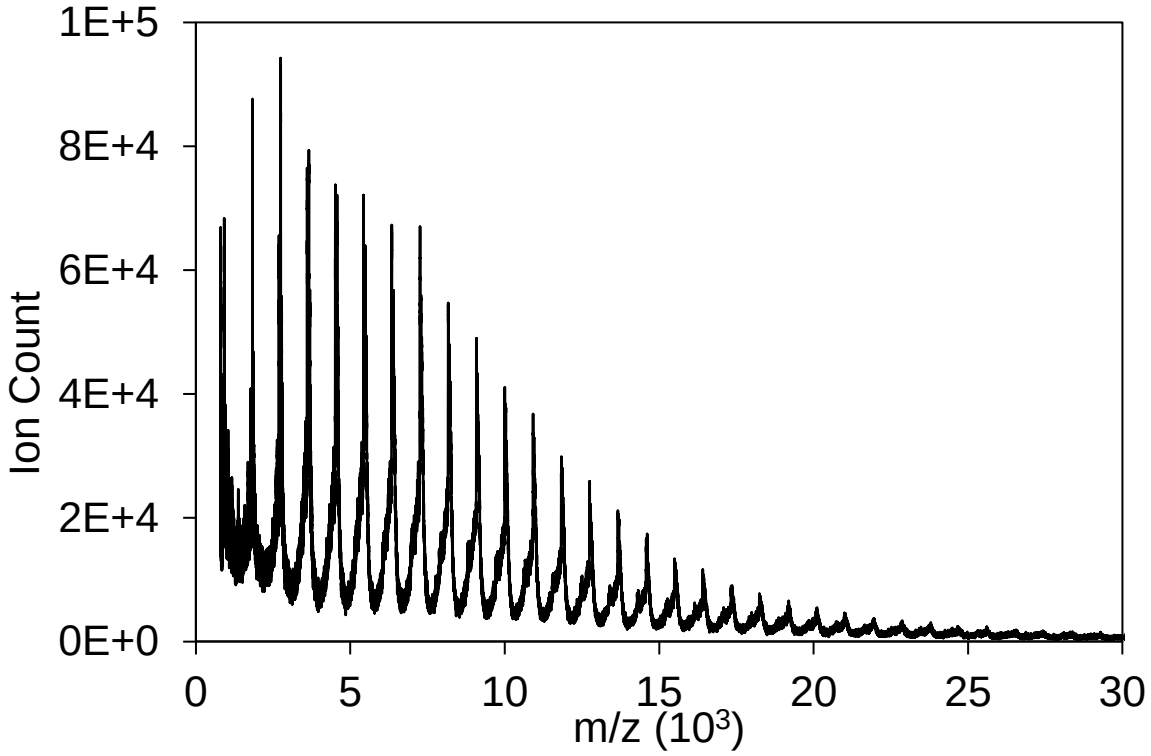


**Figure S8.** MALDI-TOF spectrum of **Poly-4**

**SEC Data for Poly-4**

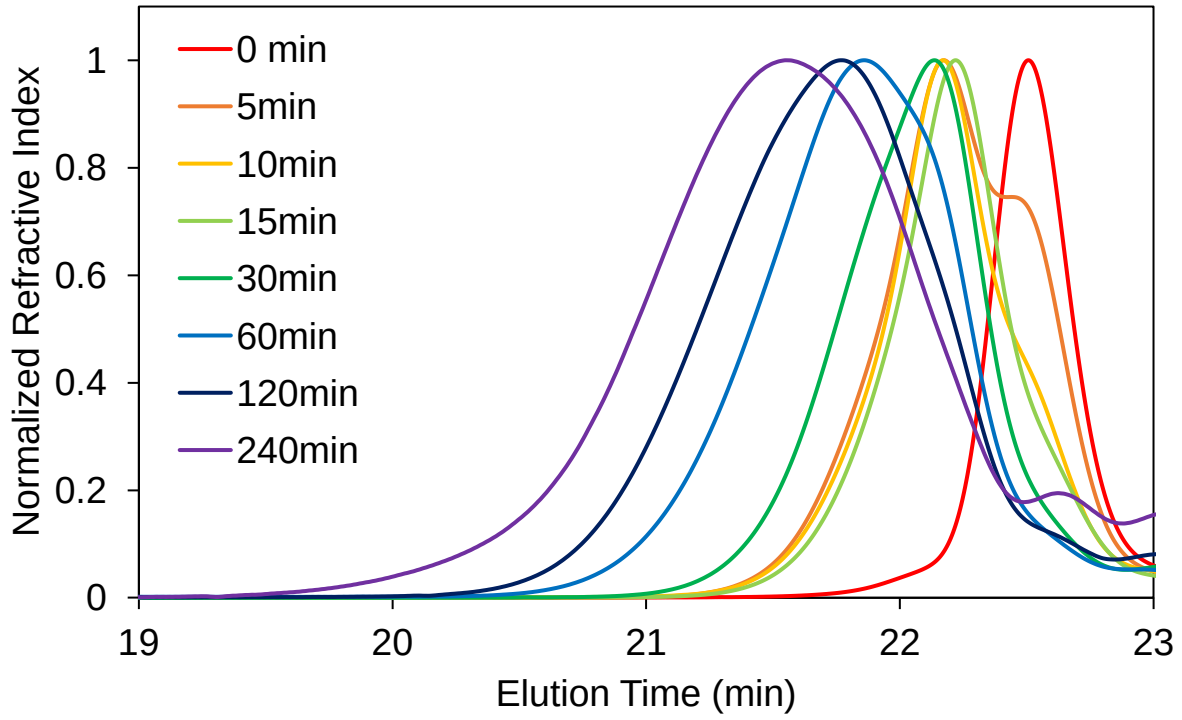


**Figure S9.** Normalized SEC curves for samples of **Poly-4** quenched at different time intervals

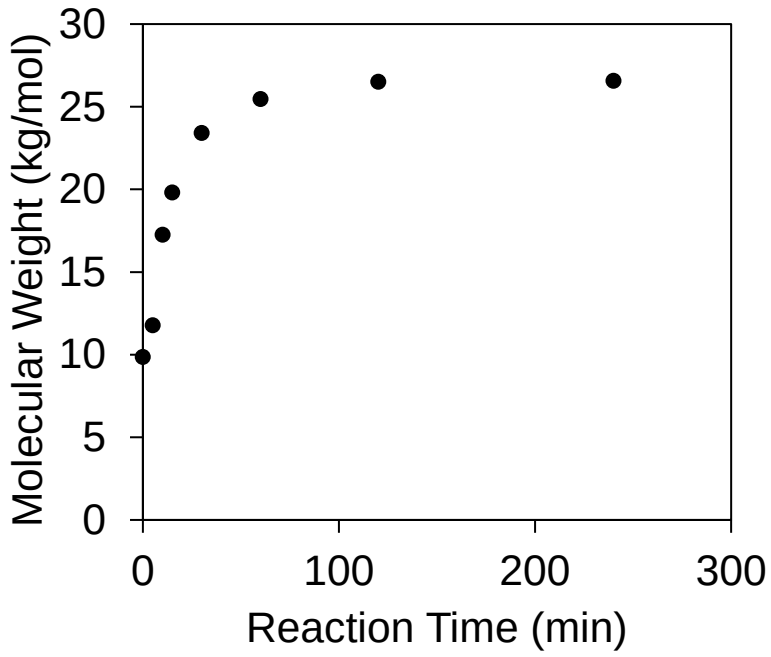


**Figure S10.** $M_{n,RALS/LALS}$ values for samples of **Poly-4**

**Photophysical Spectra**

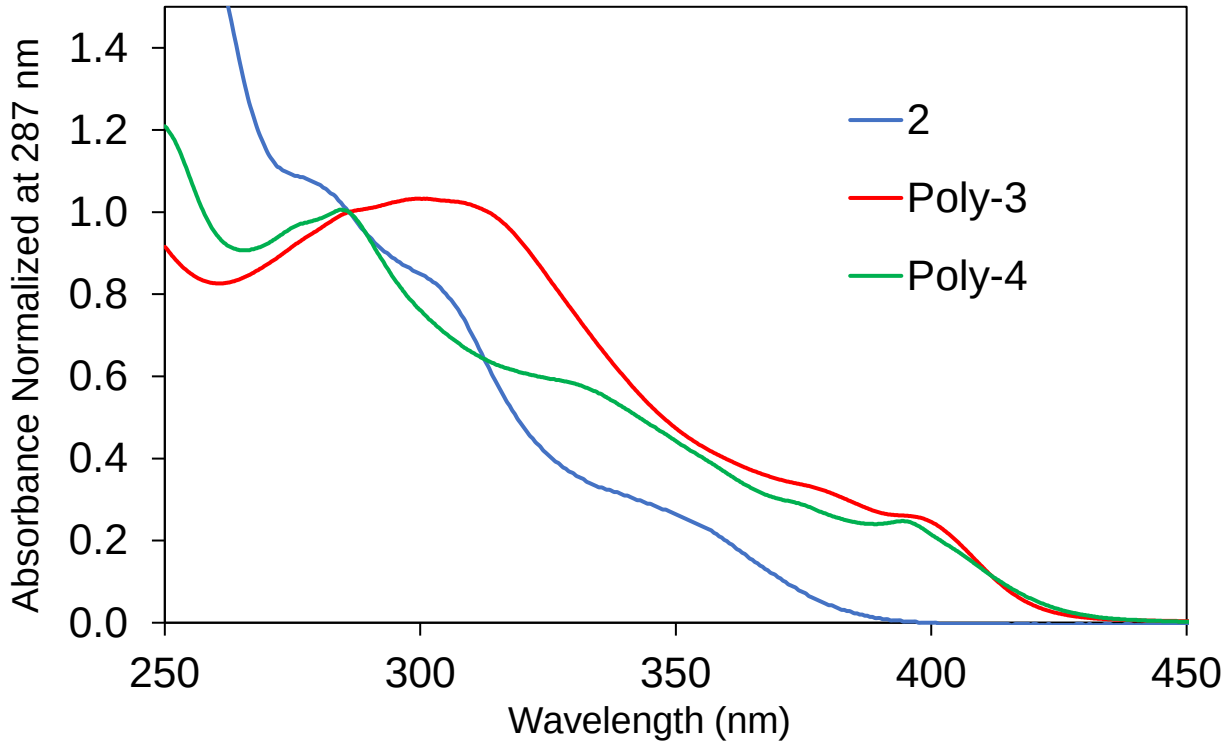


**Figure S11.** Absorbance spectra for **2** (blue), **Poly-3** (red), and **Poly-4** (green) in DCM

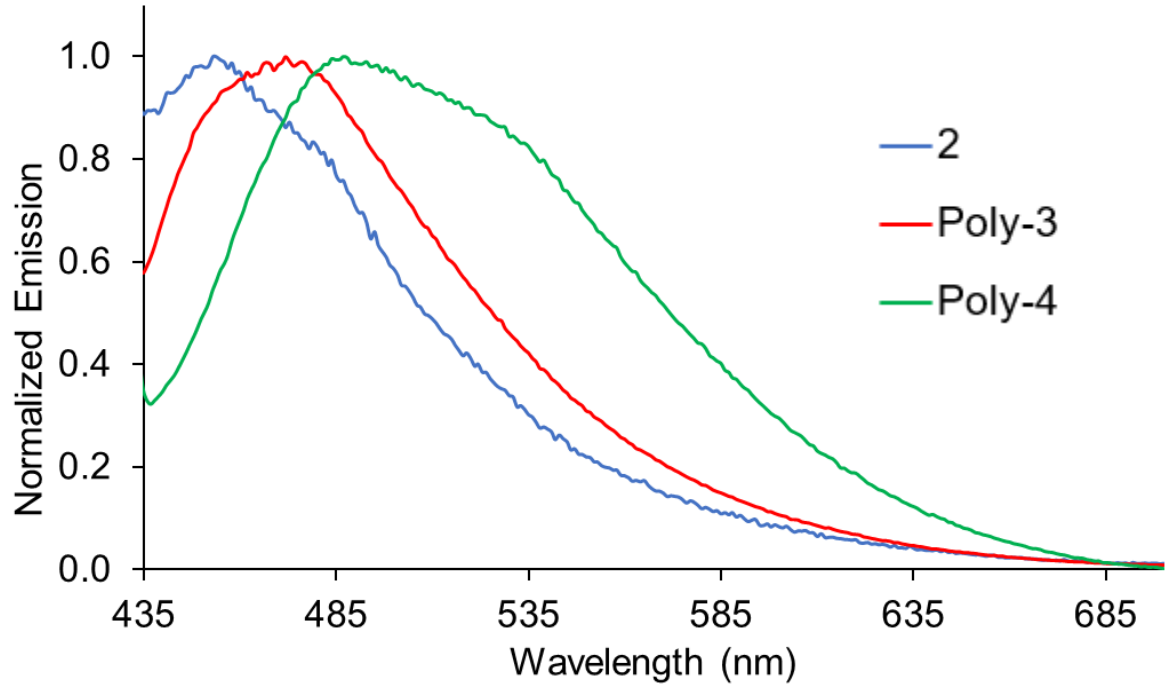


**Figure S12.** Emission spectra normalized at maximum intensity for **2** (blue, excitation at 380 nm) as well as **Poly-3** (red, excitation at 420 nm) and **Poly-4** (green, excitation at 420 nm)

**Chain Length Dependent UV-Vis Data for Poly-4**

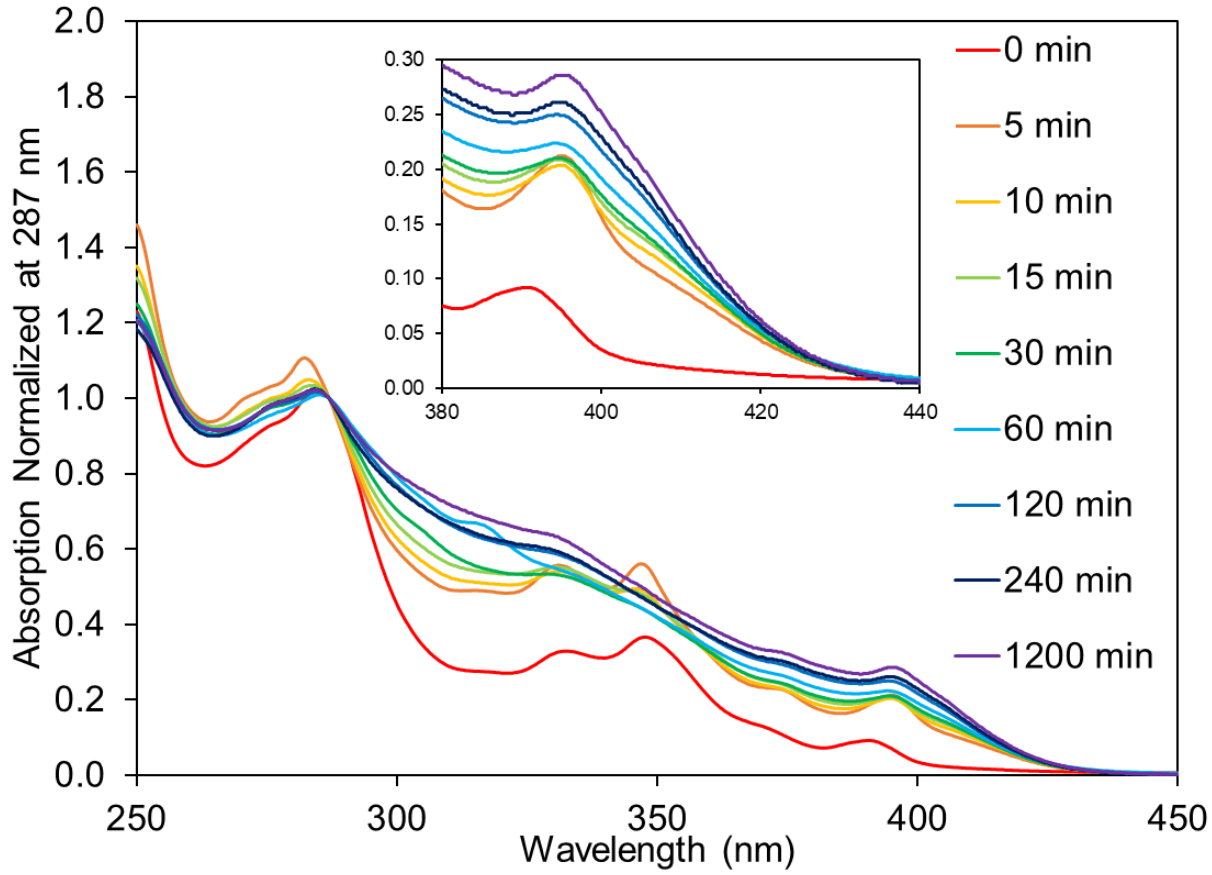


**Figure S13.** Absorption Spectra for samples of **Poly-4** normalized at 287 nm

**Thermal Gravimetric Analysis**

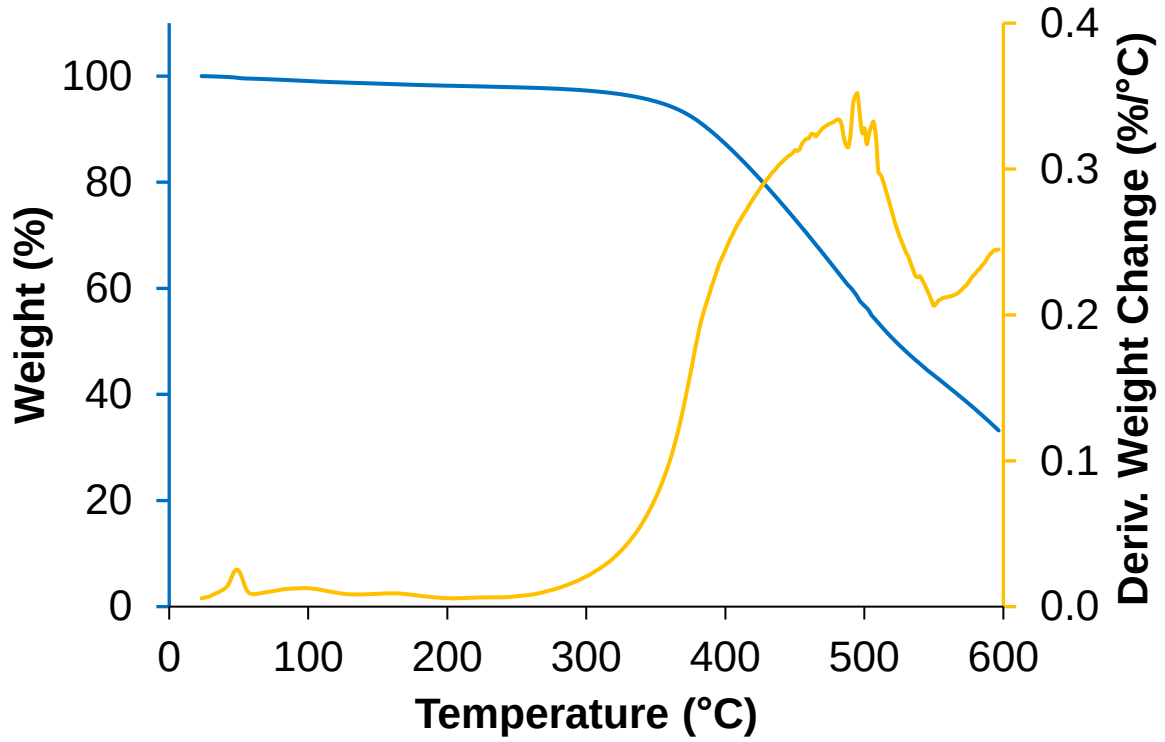


**Figure S14.** TGA Trace for **Poly-3**

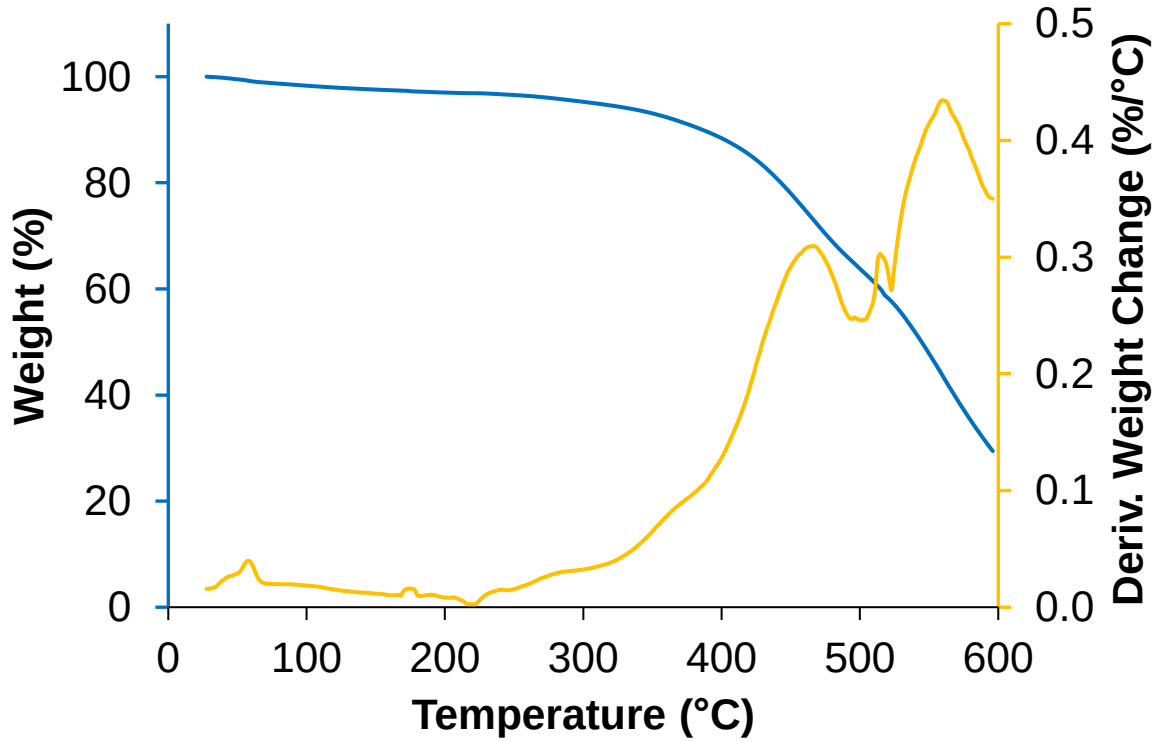


**Figure S15.** TGA Trace for **Poly-4**

**Differential Scanning Calorimetry**

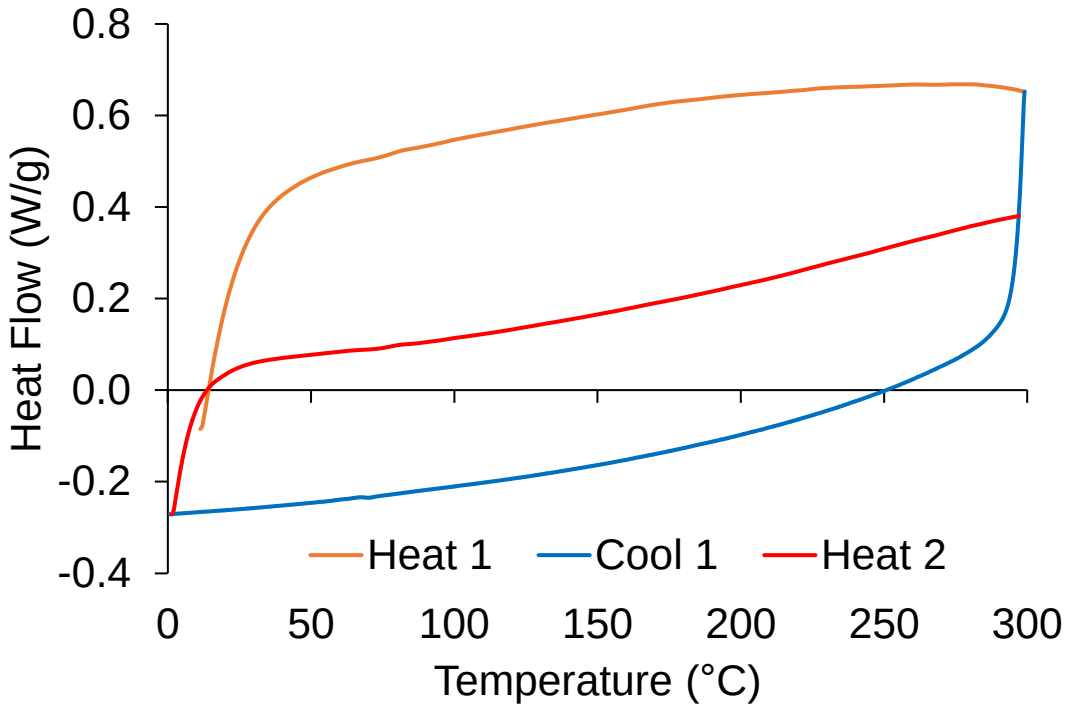


**Figure S16.** DSC Trace for **Poly-3**

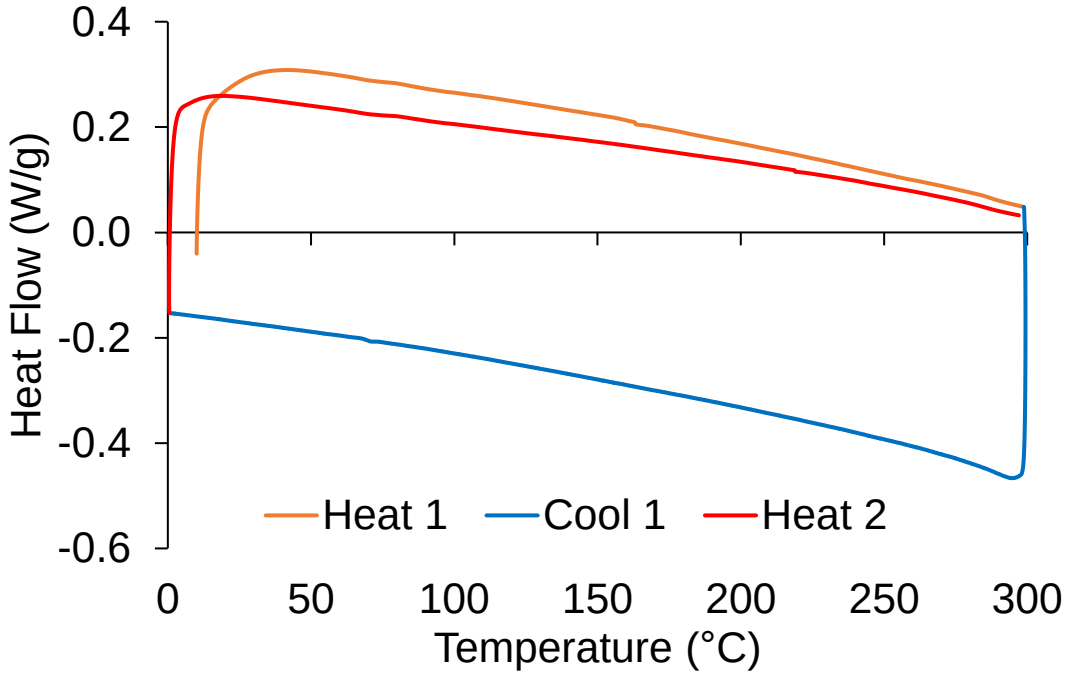


**Figure S17.** DSC Trace for **Poly-4**

## Cyclic Voltammetry

Electrochemical experiments were performed at ambient temperature. A 3 mm diameter glassy carbon electrode was used as the working electrode, with platinum and silver wires used as the counter and reference electrodes, respectively. Tetrabutylammonium hexafluorophoasphate (0.1 M) was used as electrolyte. Ferrocene was added at the end of each experiment as an internal reference against the half-potential of $Fc/Fc^{+}$. Compound **2** at a concentration of 1.0 M was measured in THF. **Poly-3** and **Poly-4** were drop-cast from DCM onto the electrode and measured in MeCN.

Compound **2** contrasts cyclooctatraene[2] and dibenz[a,e]cyclooctatetraene[3] both which show two reversible reductions. A likely cause for the behavior of **2** is found in the asymmetrical substitution pattern observed in the crystal structure which shows both phenanthrene and o-quinodimethane character.[1] Considering that isolated o-quinodimethane moieties are highly reactive, the group is likely not stable to electrochemical reduction.[4,5] Additionally, studies by Esser found that some polyolefins with COT substituents did not share reversible reductions of their monomer counterparts, attributed to partial dissolution of the polymers.[3]

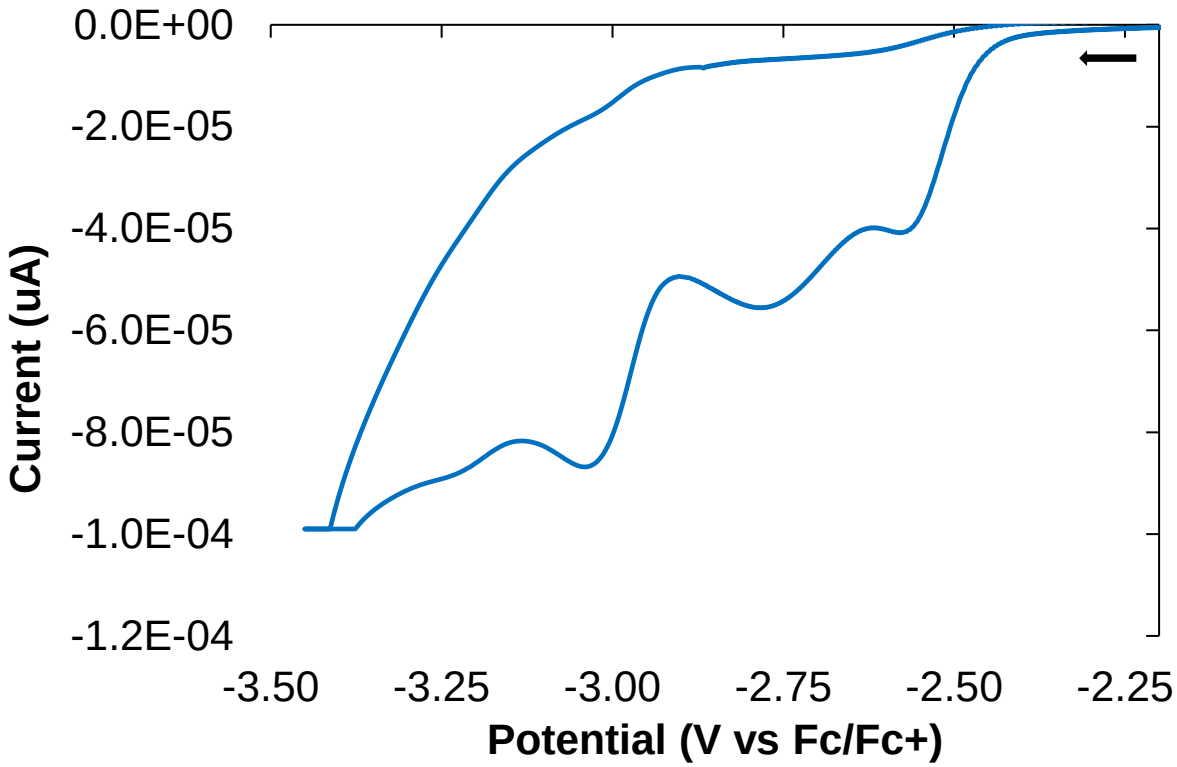


**Figure S18.** Cyclic voltammogram for **2** at concentration of 1 mM in THF at scan rate of 100 mV/s.

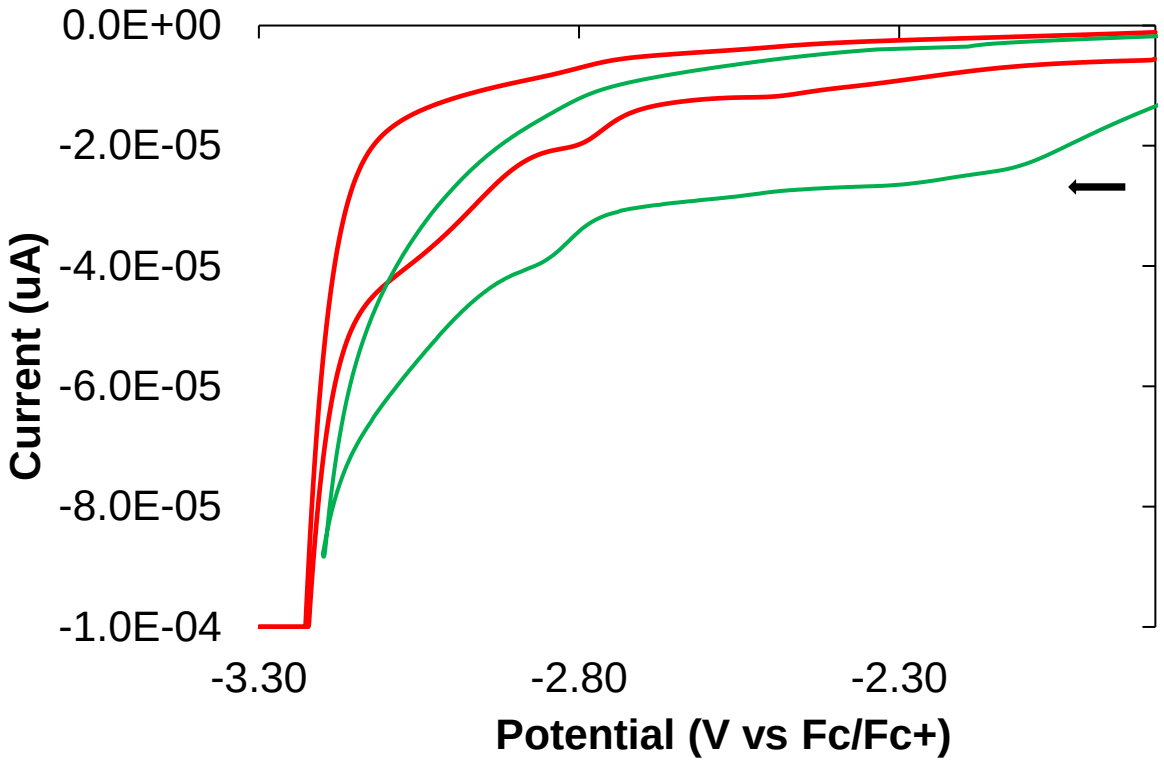


**Figure S19.** Cyclic voltammogram for **Poly-3** (red) and **Poly-4** (green). Data was acquired in MeCN with 0.1 M $NBu_4PF_6$ at at a scan rate of 100 mV/s.

**Porosimetry**

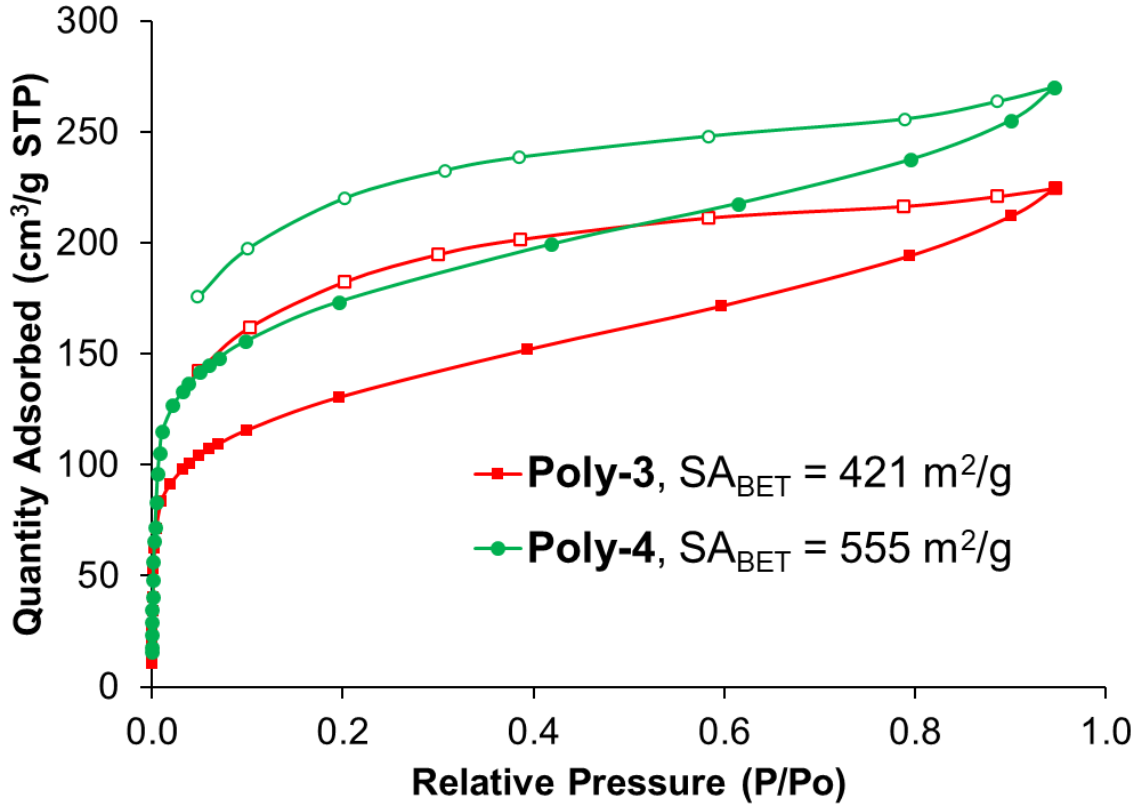


**Figure S20**. Nitrogen adsorption (filled) and desorption (open) isotherms for **Poly-3** (red) and **Poly-4** (green)

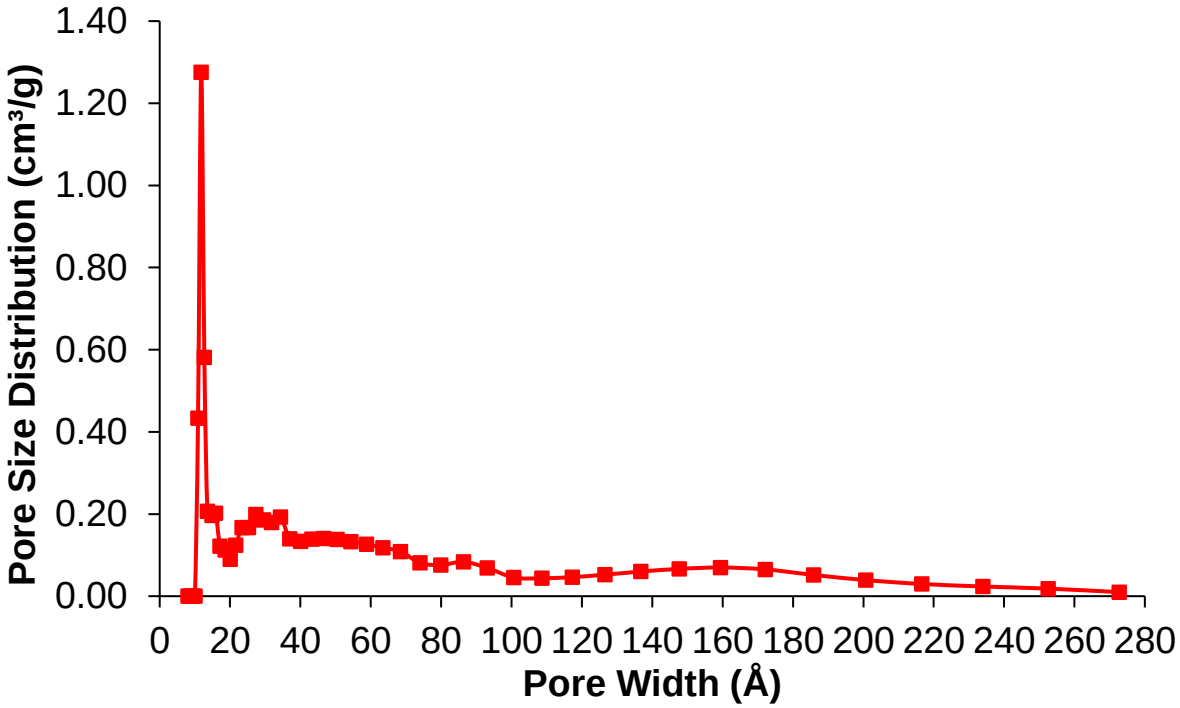


**Figure S21.** Pore size distribution for **Poly-3**

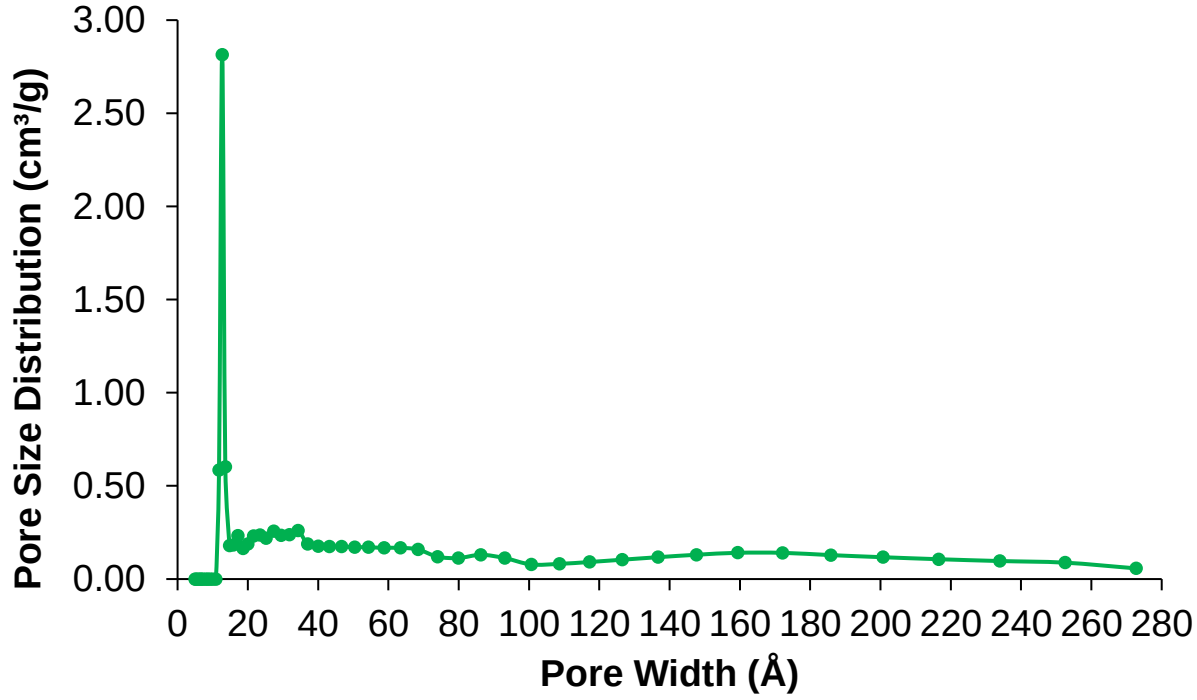


**Figure S22.** Pore size distribution for **Poly-4**

**Casting of Thin Films and Dielectric Measurement Details**

Tetrahydrofuran (THF), dimethylformamide (DMF), and chloroform were procured from Sigma-Aldrich and utilized as received without further purification. Indium tin oxide (ITO) coated glass substrates (2-3 Ω/sq, Thin Film Devices Inc., USA) underwent a thorough cleaning process with soapy water, deionized (DI) water, acetone, and isopropanol, sequentially. The substrates were then heated to 100 ºC for at least four hours, followed by ultraviolet/ozone (UV/$O_3$) treatment for 20 minutes prior to use. Pre-dried COT polymer powders were dissolved in a mixture of THF/DMF/chloroform (9:0.9:0.1) to create a 10 mg/mL solution. The solutions underwent overnight magnetic stirring.

For each drop-cast film, approximately 100 µL of the solution was deposited on a ~1.5 cm square ITO-coated glass substrate. To slow the drying process, the substrate was sealed within an overturned 125 mL glass jar, accompanied by a 6–10 mL reservoir of pure THF solvent placed in small lids at the jar's four edges. The jar, along with the substrate, was placed in an air-drying oven with the lowest adjusted flow rate, allowing the solution to slowly dry for 4 hours. Subsequently, a silicon wafer was inserted into the jar, creating an incompletely closed environment, to facilitate the evaporation of the remaining solvents on the ITO substrate. After 4 hours, the four small lids with THF solvent were swiftly removed, and the temperature of the air-drying oven was gradually increased to 60 ºC with the silicon wafer still inserted. After 12 hours, the oven temperature was reset to room temperature. Once the oven reached room temperature, the samples were removed from the jar and transferred to a vacuum oven for 12 hours to completely remove solvent residuals and moisture. The typical thickness of the COT polymer films ranged between 2 µm and 4 µm, verified using a Dektak 3030ST profilometer.

For electrical measurements, gold electrodes (~30 nm thick) were deposited on the top surface of the COT polymer films using a magnetron sputter (Q150R, Quorum). Silver paint (Leitsilber 200, TED PELLA, USA) was employed to ensure electrical contact between the polymer film and ITO layer, as well as electrically ground the ITO layer. The electrode area for dielectric spectra measurements was 10 $mm^2$, and for dielectric breakdown and electric displacement-electric field (D-E) loop measurements was 4 $mm^2$. Frequency-dependent dielectric spectra of the film samples were recorded over the frequency range of 500 Hz to 105 Hz using a Hewlett Packard 4284A LCR meter. Dielectric breakdown strengths were measured utilizing a Trek 610D instrument amplifier as the voltage source based on an electrostatic pull-down method, applying a DC voltage ramp of 200 V/s to the film samples until dielectric failure occurred. Electric displacement-electric field (D-E) loops were obtained under varied applied electric fields using a modified Sawyer-Tower circuit, integrated with a PK-CPE1801 high-voltage test system from PolyK Technologies, LLC., USA. Voltages with a unipolar triangular waveform were applied at a frequency of 100 Hz. Discharged energy density and energy efficiency were calculated based on the obtained D-E loops.

**Grazing-Incidence Wide-Angle X-ray Scattering**

GIWAXS measurements was conducted on beamline 7.3.3 at the Advanced Light Source at Berkeley Lawrence National Lab. Data was collected under a helium environment with an incident beam energy of 10 keV and an incidence angle of 0.14°. Thin film samples were spin-cast on Si wafers. The scattering signal was collected by a Pilatus 2Mdetector and processed using Igor 8 software combined with Nika package and WAXSTools.

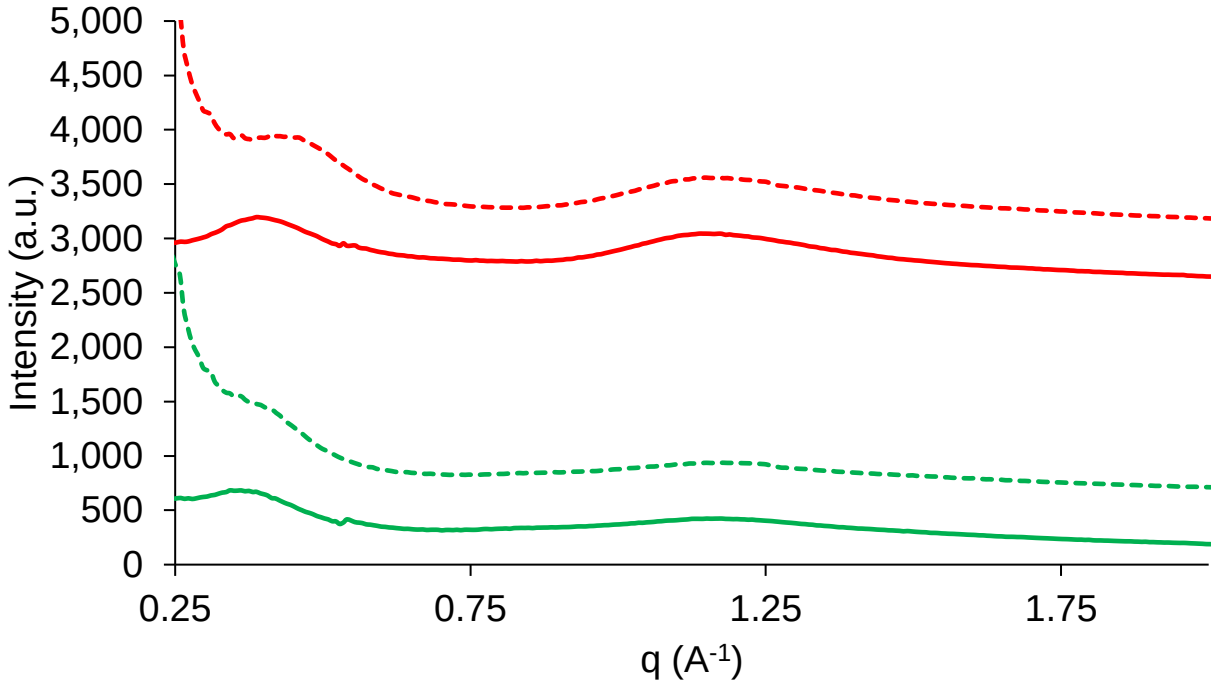


**Figure S23.** 1D GIWAXS cut for **Poly-3** (red; solid, in plane; dotted, out of plane) and **Poly-4** (green; solid, in plane; dotted, out of plane)

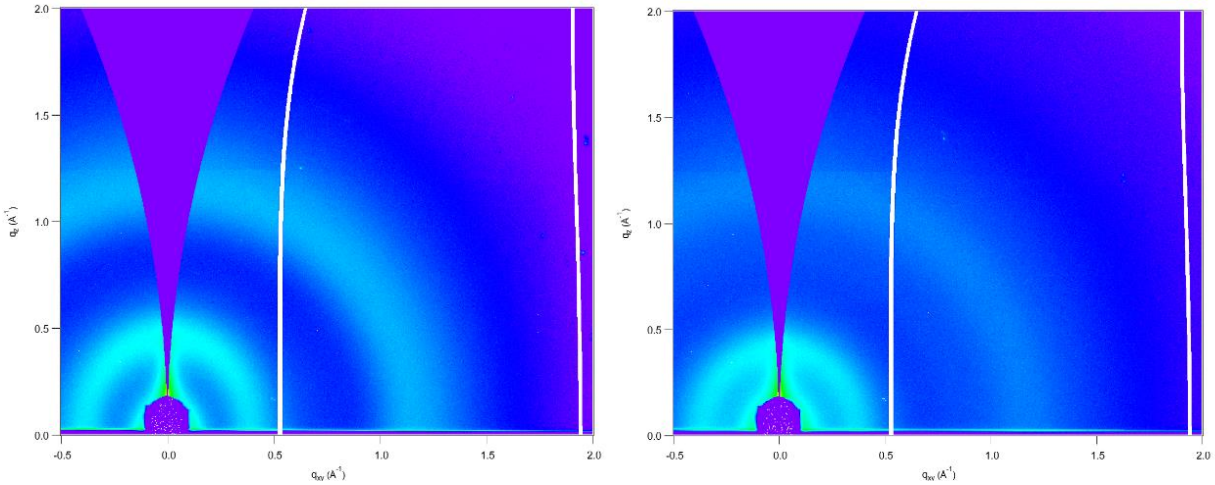

**Figure S24.** GIWAXS diffraction pattern **Poly-3** (left) and **Poly-4** (right)

**Dielectric Breakdown**

The dielectric breakdown strength of the polymer-based films was assessed using a two-parameter Weibull statistic model, denoted as $P(E) = 1 - \exp(-(E_b/\alpha)^{\beta})$. Here, $P(E)$ is the cumulative probability of electric failure, $E_b$ is the measured electrical breakdown field, $\alpha$ is the field strength corresponding to a 63.2% probability of dielectric breakdown failure (i.e., Weibull E*b*), and $\beta$ gauges the scatter of the data. High values of $\beta$ indicate less scattering in the experimental data. Statistical analysis reveals that both polymer films exhibit high Weibull E*b* and reasonably large $\beta$, i.e., 637.76 MV/m and 11.21 for **Poly-4** versus 552.09 MV/m and 13.11 for **Poly-3** (Figure S#), indicating their suitability for use in dielectric capacitors operating under high voltages.

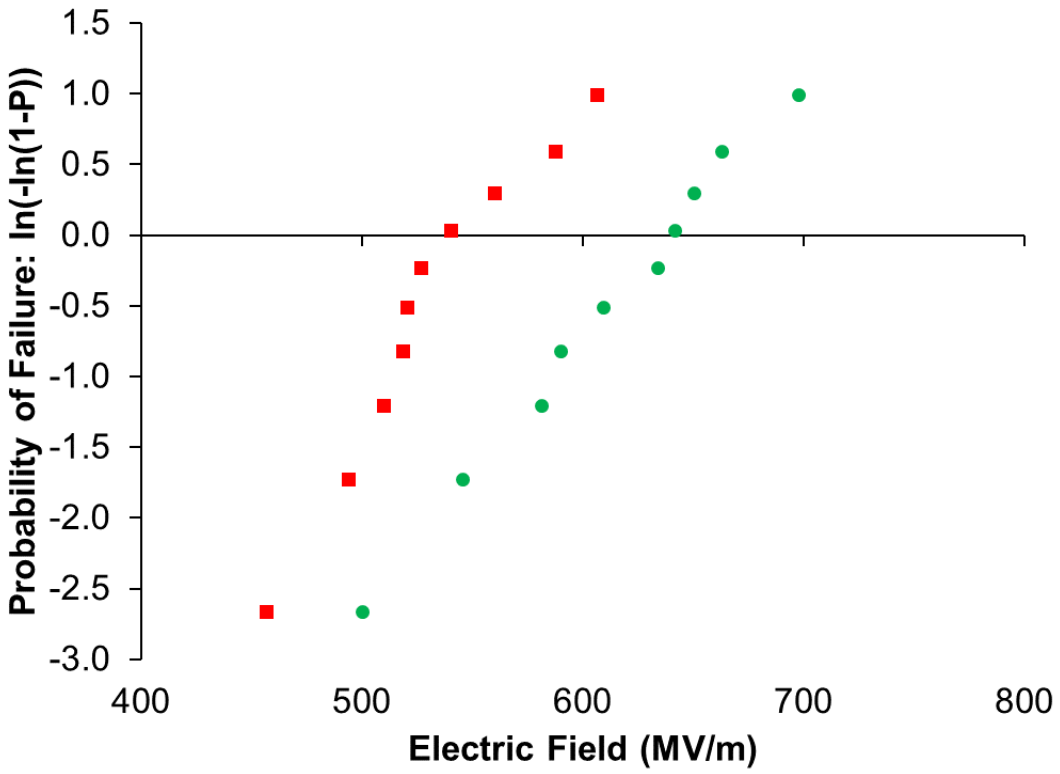


**Figure S25.** Dielectric breakdown plot for **Poly-3** (red) and **Poly-4** (green)

## Density Functional Theory

### Ground State Geometry Optimizations

Density functional theory (DFT) calculations of **2** were performed using Gaussian 16 Revision C.01.[6] Molecular geometry was optimized at the B3LYP/6-31g level of theory. All optimization was carried out in unconstrained C1 symmetry, and all geometries were confirmed to be local minima by normal mode frequency calculations. The structure was visualized using Mercury 4.0.[7]

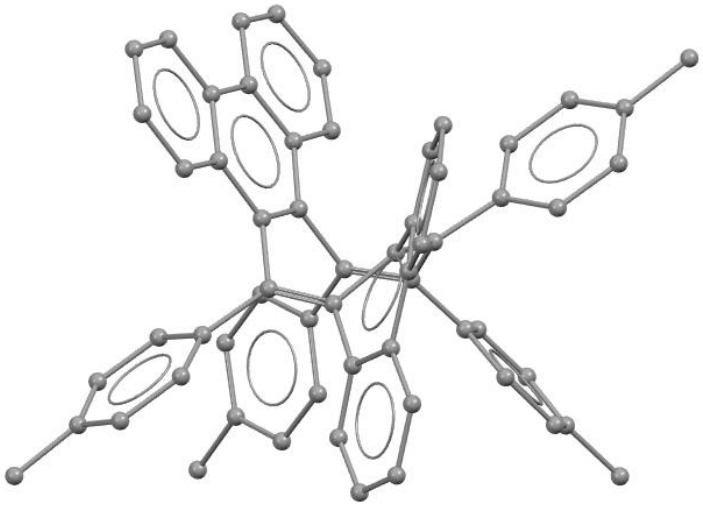

**Figure S26.** DFT-Optimized structure for **2**. Hydrogen atoms omitted for clarity.

| | | | | | | | |
|---|---|---|---|---|---|---|---|
| C | 0.75930 | -1.41900 | -0.42840 | C | -3.44380 | -2.87900 | 4.09810 |
| C | -0.58790 | -1.12590 | -1.01650 | C | -2.61610 | -1.84650 | 4.50680 |
| C | -1.65290 | -0.70330 | -0.27590 | C | -0.72030 | 0.27690 | 5.35800 |
| C | -1.45840 | -0.43640 | 1.19050 | C | 0.19680 | 1.24350 | 5.73910 |
| C | -0.59710 | 0.55960 | 1.59080 | C | 0.87930 | 1.99080 | 4.75930 |
| C | 0.07560 | 1.43920 | 0.56500 | C | 0.62000 | 1.76220 | 3.41810 |
| C | 1.21260 | 0.99120 | -0.04740 | C | 0.11960 | -3.03030 | -4.20360 |
| C | 1.61590 | -0.45170 | 0.01880 | C | -0.46710 | -2.21710 | -5.17570 |
| C | -2.12830 | -1.27220 | 2.17730 | C | -1.10700 | -1.02880 | -4.80040 |
| C | -1.92960 | -1.02940 | 3.57290 | C | -1.16900 | -0.66590 | -3.45300 |
| C | -1.00270 | 0.01380 | 3.99310 | C | 1.67210 | -3.62570 | 0.45380 |
| C | -0.32370 | 0.78490 | 2.99980 | C | 1.90240 | -4.99300 | 0.28500 |
| C | 1.07700 | -2.86780 | -0.56790 | C | 1.53650 | -5.62180 | -0.91170 |
| C | 0.69670 | -3.50520 | -1.78230 | C | 0.93600 | -4.88190 | -1.93280 |
| C | 0.06860 | -2.68220 | -2.84230 | C | 3.02880 | -0.72780 | 0.43280 |
| C | -0.59920 | -1.48430 | -2.46310 | C | 2.11580 | 1.85870 | -0.86650 |
| C | -2.95850 | -2.35620 | 1.78890 | C | -0.60540 | 2.73180 | 0.24940 |
| C | -3.60710 | -3.14360 | 2.72490 | C | -3.03850 | -0.52730 | -0.81300 |

| | | | | | | | |
|---|---|---|---|---|---|---|---|
| C | -3.78730 | 0.60900 | -0.45260 | H | -1.54610 | -0.38310 | -5.55420 |
| C | -5.09200 | 0.78900 | -0.92030 | H | -1.65740 | 0.25640 | -3.16020 |
| C | -5.70500 | -0.16160 | -1.75150 | H | 1.94510 | -3.13950 | 1.38290 |
| C | -4.96490 | -1.30740 | -2.09430 | H | 2.35430 | -5.56680 | 1.08770 |
| C | -3.65920 | -1.48820 | -1.63790 | H | 1.70480 | -6.68610 | -1.04290 |
| C | 3.93230 | -1.41580 | -0.39890 | H | 0.62830 | -5.38320 | -2.84470 |
| C | 5.25230 | -1.63130 | -0.00060 | H | -3.34200 | 1.35830 | 0.19290 |
| C | 5.72300 | -1.16860 | 1.24070 | H | -5.64330 | 1.67920 | -0.62990 |
| C | 4.82220 | -0.48020 | 2.06880 | H | -5.42090 | -2.07030 | -2.71980 |
| C | 3.50170 | -0.25440 | 1.67020 | H | -3.11820 | -2.38710 | -1.91190 |
| C | 2.58450 | 3.09420 | -0.37940 | H | 3.59690 | -1.78060 | -1.36350 |
| C | 3.45110 | 3.88350 | -1.13570 | H | 5.92950 | -2.16330 | -0.66370 |
| C | 3.88490 | 3.47300 | -2.40890 | H | 5.15800 | -0.11540 | 3.03590 |
| C | 3.42630 | 2.23650 | -2.89090 | H | 2.82620 | 0.28030 | 2.33040 |
| C | 2.56370 | 1.43990 | -2.13320 | H | 2.26820 | 3.43380 | 0.60120 |
| C | -0.65990 | 3.21070 | -1.07950 | H | 3.80300 | 4.82890 | -0.73110 |
| C | -1.35200 | 4.37630 | -1.40270 | H | 3.75100 | 1.89150 | -3.86880 |
| C | -2.02990 | 5.12050 | -0.42050 | H | 2.22400 | 0.48850 | -2.52990 |
| C | -2.00210 | 4.63540 | 0.89560 | H | -0.16600 | 2.65220 | -1.86510 |
| C | -1.31380 | 3.46410 | 1.22540 | H | -1.37770 | 4.70880 | -2.43720 |
| C | -7.10970 | 0.04250 | -2.27380 | H | -2.53020 | 5.17740 | 1.67550 |
| C | 7.16230 | -1.38090 | 1.65530 | H | -1.32810 | 3.12210 | 2.25280 |
| C | 4.80370 | 4.34500 | -3.23580 | H | -7.67460 | 0.73530 | -1.64140 |
| C | -2.75560 | 6.39920 | -0.77350 | H | -7.10120 | 0.46010 | -3.29020 |
| H | -3.08840 | -2.56990 | 0.73750 | H | -7.66260 | -0.90260 | -2.31810 |
| H | -4.23840 | -3.96390 | 2.39870 | H | 7.53770 | -2.35400 | 1.31880 |
| H | -3.95550 | -3.48850 | 4.83620 | H | 7.81960 | -0.61350 | 1.22340 |
| H | -2.49100 | -1.67310 | 5.56860 | H | 7.27630 | -1.33270 | 2.74340 |
| H | -1.22300 | -0.29120 | 6.13090 | H | 5.56930 | 4.82350 | -2.61430 |
| H | 0.39200 | 1.41920 | 6.79210 | H | 5.31340 | 3.76500 | -4.01210 |
| H | 1.60480 | 2.74260 | 5.05320 | H | 4.24750 | 5.14830 | -3.73860 |
| H | 1.14340 | 2.33610 | 2.66270 | H | -2.05560 | 7.23970 | -0.87840 |
| H | 0.64560 | -3.92950 | -4.50710 | H | -3.29200 | 6.30690 | -1.72500 |
| H | -0.40980 | -2.49910 | -6.22230 | H | -3.48190 | 6.67330 | -0.00130 |

**Table S2.** Cartesian coordinates for **2**. From left to right: x, y, z in Å.

**Calculated Stretching Frequencies**

Vibrational frequencies were calculated at the B3LYP/6-31g level of theory on the optimized structure of **2**. To account for general discrepancies between the observed FTIR spectra for **2**, a correction factor of -60 $cm^{-1}$ was applied to the calculated spectra from 500 to 2000 $cm^{-1}$ and a correction factor of -170 $cm^{-1}$ was applied to the calculated spectra from 2000 to 3500 $cm^{-1}$.

**Comparison of Crystal Structure and DFT-Optimized Geometry**

Hydrogen atoms were removed from the crystallographically determined and DFT-optimized structure of **2** and they were overlayed using Mercury 4.0.[7] The calculated root mean squared deviation was 0.2654 Å.

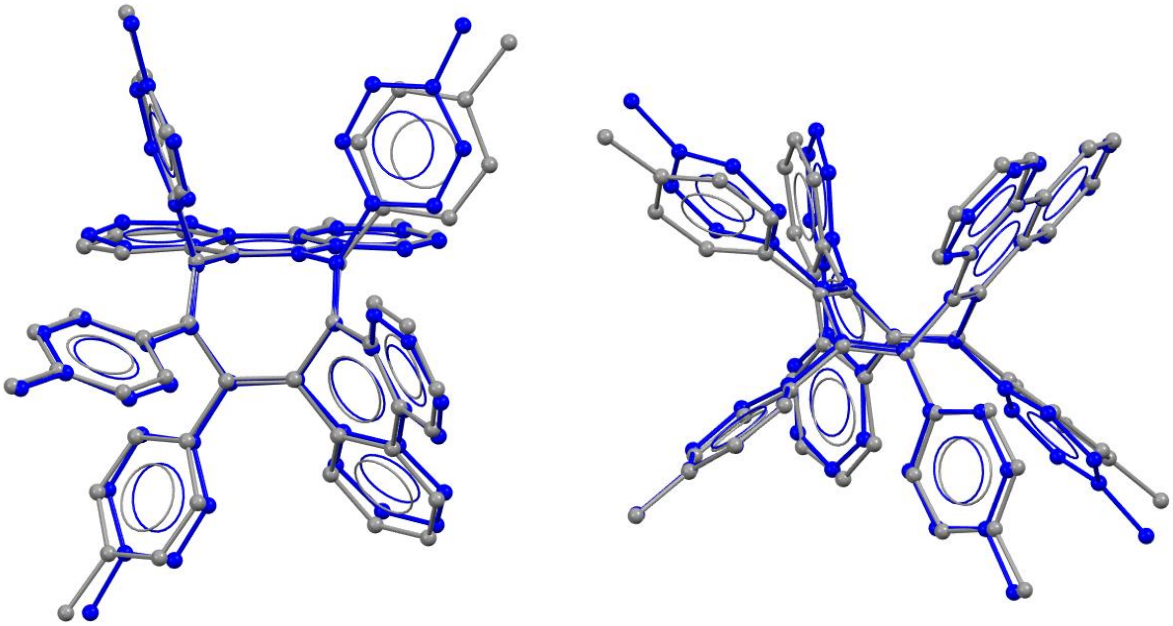

**Figure S27.** Comparison of DFT-optimized (B3LYP/6-31g) (blue) and crystallographically determined (gray) structures of **2**.

## References


(1) Bergman, H. M.; Beattie, D. D.; Kiel, G. R.; Handford, R. C.; Liu, Y.; Tilley, T. D. A Sequential Cyclization/π-Extension Strategy for Modular Construction of Nanographenes Enabled by Stannole Cycloadditions. *Chem. Sci.* **2022**, *13* (19), 5568–5573. https://doi.org/10.1039/D2SC00397J.

(2) Allendoerfer, R. D. Mechanism of the Electrochemical Reduction of Cyclooctatetraene. *J. Am. Chem. Soc.* **1975**, *97* (1), 218–219. https://doi.org/10.1021/ja00834a054.

(3) Desmaizieres, G.; Speer, M. E.; Thiede, I.; Gaiser, P.; Perner, V.; Kolek, M.; Bieker, P.; Winter, M.; Esser, B. Dibenzo[a,e]Cyclooctatetraene-Functionalized Polymers as Potential Battery Electrode Materials. *Macromol. Rapid Commun.* **2021**, *42* (18), 2000725. https://doi.org/10.1002/marc.202000725.

(4) Kiel, G. R.; Ziegler, M. S.; Tilley, T. D. Zirconacyclopentadiene-Annulated Polycyclic Aromatic Hydrocarbons. *Angew. Chem. Int. Ed.* **2017**, *56* (17), 4839–4844. https://doi.org/10.1002/anie.201700818.

(5) Segura, J. L.; Martín, N. O-Quinodimethanes: Efficient Intermediates in Organic Synthesis. *Chem. Rev.* **1999**, *99* (11), 3199–3246. https://doi.org/10.1021/cr990011e.

(6) Frisch, M. J.; Trucks, G. W.; Schlegel, H. B.; Scuseria, G. E.; Robb, M. A.; Cheeseman, J. R.; Scalmani, G.; Barone, V.; Petersson, G. A.; Nakatsuji, H.; Li, X.; Caricato, M.; Marenich, A. V.; Bloino, J.; Janesko, B. G.; Gomperts, R.; Mennucci, B.; Hratchian, H. P.; Ortiz, J. V.; Izmaylov, A. F.; Sonnenberg, J. L.; Williams; Ding, F.; Lipparini, F.; Egidi, F.; Goings, J.; Peng, B.; Petrone, A.; Henderson, T.; Ranasinghe, D.; Zakrzewski, V. G.; Gao, J.; Rega, N.; Zheng, G.; Liang, W.; Hada, M.; Ehara, M.; Toyota, K.; Fukuda, R.; Hasegawa, J.; Ishida, M.; Nakajima, T.; Honda, Y.; Kitao, O.; Nakai, H.; Vreven, T.; Throssell, K.; Montgomery Jr., J. A.; Peralta, J. E.; Ogliaro, F.; Bearpark, M. J.; Heyd, J. J.; Brothers, E. N.; Kudin, K. N.; Staroverov, V. N.; Keith, T. A.; Kobayashi, R.; Normand, J.; Raghavachari, K.; Rendell, A. P.; Burant, J. C.; Iyengar, S. S.; Tomasi, J.; Cossi, M.; Millam, J. M.; Klene, M.; Adamo, C.; Cammi, R.; Ochterski, J. W.; Martin, R. L.; Morokuma, K.; Farkas, O.; Foresman, J. B.; Fox, D. J. Gaussian 16 Rev. C.01, 2016.

(7) *(IUCr) Mercury 4.0: from visualization to analysis, design and prediction*. https://journals.iucr.org/j/issues/2020/01/00/gj5232/index.html (accessed 2024-09-11).